Report

Current Biology

# Local Inversion Heterozygosity Alters Recombination throughout the Genome

## Highlights

- Heterozygous inversions shift the crossover landscape (the interchromosomal effect)
- Crossovers on freely recombining chromosomes increase and noncrossovers decrease
- Unlike crossovers, noncrossovers are not suppressed by inversion breakpoints
- The interchromosomal effect does not increase the number of double-strand breaks

## Authors

K. Nicole Crown, Danny E. Miller, Jeff Sekelsky, R. Scott Hawley

## Correspondence

rsh@stowers.org

## In Brief

Heterozygous inversions suppress crossing over during meiosis while increasing crossover frequency elsewhere in the genome. Crown et al. show that noncrossover frequency decreases on chromosomes able to undergo exchange, inversion breakpoints do not suppress noncrossovers, and inversions alter genome-wide double-strand break repair outcomes.

Crown et al., 2018, Current Biology *28*, 2984–2990
September 24, 2018 
https://doi.org/10.1016/j.cub.2018.07.004

CellPress

CellPress

Current Biology
Report

# Local Inversion Heterozygosity Alters Recombination throughout the Genome

K. Nicole Crown,[1,2,3,6,7] Danny E. Miller,[4,5,6,8] Jeff Sekelsky,[1,2,3] and R. Scott Hawley[4,5,9,*]
[1]Integrative Program for Biological and Genome Sciences, University of North Carolina at Chapel Hill, Chapel Hill, NC, USA
[2]Department of Biology, University of North Carolina at Chapel Hill, Chapel Hill, NC, USA
[3]Lineberger Comprehensive Cancer Center, University of North Carolina at Chapel Hill, Chapel Hill, NC, USA
[4]Stowers Institute for Medical Research, Kansas City, MO, USA
[5]MD-PhD Physician Scientist Training Program, University of Kansas Medical Center, Kansas City, KS, USA
[6]These authors contributed equally
[7]Present address: Department of Biology, Case Western Reserve University, Cleveland, OH, USA
[8]Present address: Department of Pediatrics, Seattle Children's Hospital and University of Washington, 4800 Sand Point Way NE, Seattle, WA 98105, USA
[9]Lead Contact
*Correspondence: rsh@stowers.org
https://doi.org/10.1016/j.cub.2018.07.004

## SUMMARY

**Crossovers (COs) are formed during meiosis by the repair of programmed DNA double-strand breaks (DSBs) and are required for the proper segregation of chromosomes. More DSBs are made than COs, and the remaining DSBs are repaired as noncrossovers (NCOs). The distribution of recombination events along a chromosome occurs in a stereotyped pattern that is shaped by CO-promoting and CO-suppressing forces, collectively referred to as crossover patterning mechanisms. Chromosome inversions are structural aberrations that, when heterozygous, disrupt the recombination landscape by suppressing crossing over. In *Drosophila* species, the local suppression of COs by heterozygous inversions triggers an increase in crossing over on freely recombining chromosomes termed the interchromosomal (IC) effect [1, 2]. The molecular mechanism(s) by which heterozygous inversions suppress COs, whether noncrossover gene conversions (NCOGCs) are similarly affected, and what mediates the increase in COs in the rest of the genome remain open questions. By sequencing whole genomes of individual offspring from mothers containing heterozygous inversions, we show that, although COs are suppressed by inversions, NCOGCs occur throughout inversions at higher than wild-type frequencies. We confirm that CO frequency increases on the freely recombining chromosomes, yet CO interference remains intact. Intriguingly, NCOGCs do not increase in frequency on the freely recombining chromosomes and the total number of DSBs is approximately the same per genome. Together, our data show that heterozygous inversions change the recombination landscape by altering the relative proportions of COs and NCOGCs and suggest that DSB fate may be plastic until a CO assurance checkpoint has been satisfied.**

## RESULTS AND DISCUSSION

To understand the molecular mechanism of the interchromosomal (IC) effect, we used whole-genome sequencing to identify crossover (CO) and noncrossover gene conversion (NCOGC) events in the presence of heterozygous, multiply inverted chromosomes in individual offspring of *D. melanogaster* females. This approach allowed us to examine rates of both COs and NCOGCs and to map these events within 100–1,000 nt of their precise breakpoints. Specifically, we generated females heterozygous for the X and 3$^{rd}$ chromosome balancers *FM7w* and *TM6B*, or the 2$^{nd}$ and 3$^{rd}$ chromosome balancers *CyO* and *TM6B* and sequenced their individual progeny (Figure 1A; Table S2). These balancer chromosomes are multiply inverted across their entire lengths and, with the exception of rare double COs, completely suppress COs [3–6]. We sequenced a total of 102 individuals to average depth of 58× (minimum: 36×; maximum: 147×), with an average SNP density of 1 SNP every 358 bp for *chrX*, 1 SNP every 239 bp for *chr2L*, and 1 SNP every 294 bp for *chr2R*. This allowed us to identify a total of 146 individual CO events and 101 NCOGC events (data for individual events are in Figures S1 and S2 and Data S1).

We first examined changes in the recombination landscape on the un-balanced, freely recombining chromosomes. As expected, by suppressing COs on heterozygous inversions, we observed a large increase in CO frequency on the freely recombining chromosomes as compared to when balancer chromosomes are not present (i.e., a wild-type genome). The map length of the X chromosome increases from 56 cM in wild-type to 140 cM ($p < 0.001$; chi-square test), and the 2$^{nd}$ chromosome increases from 104 cM in wild-type to 140 cM ($p = 0.02$; chi-square test; Figure 1B; Table S1; Data S1). Although both chromosomes experience statistically significant changes in CO distribution (Kolmogorov-Smirnov test; *chrX* $p = 0.05$; *chr2* $p < 0.05$), the X chromosome has a larger, non-uniform increase in CO frequency than chromosome *2*, with disproportionately

 

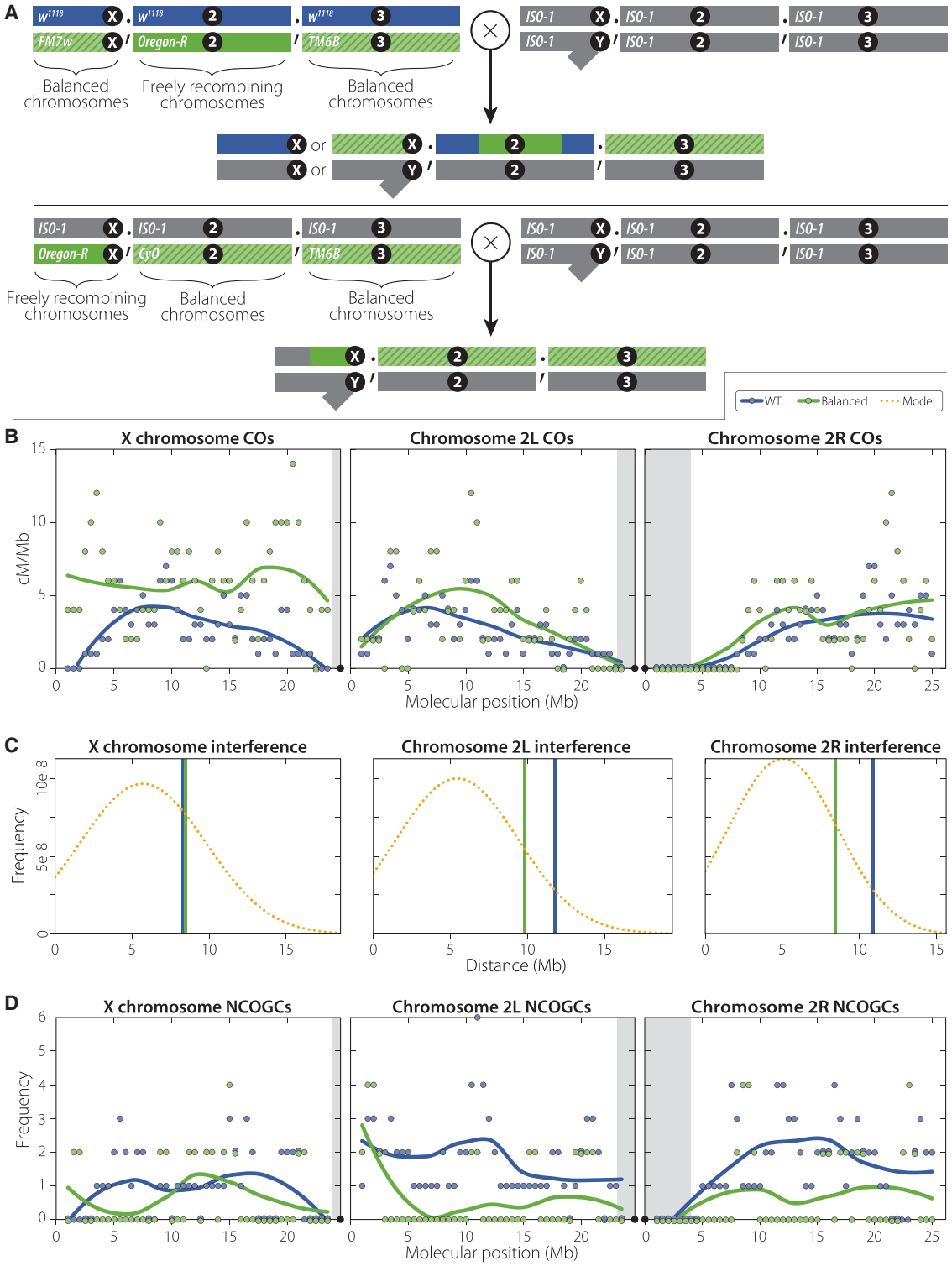


**Figure 1. Frequency and Distribution of Recombination Events on Freely Recombining Normal-Sequence Chromosomes in the Presence of Heterozygous Inversions**

(A) Cross scheme showing the genotypes used in this study. Multiply inverted balancer chromosomes are depicted with hashes, and structurally linear (normal sequence) chromosomes are solid. The multiply inverted balancer chromosomes suppress COs between that pair of chromosomes and cause the interchromosomal effect during which the normal sequence chromosomes experience an increase in CO frequency. Recombination on the X chromosome was analyzed in a different genetic background than chromosome *2* because the SNP density between $w^{1118}$ and *Oregon-R* was too low to analyze NCOGCs.

*(legend continued on next page)*

**Table 1. Expected and Observed Frequencies of Recombination Events on Freely Recombining Chromosomes in the Presence of Heterozygous Inversions**

| | *ChrX* | | *Chr2L* | | *Chr2R* | |
|---|---|---|---|---|---|---|
| | Expected | Observed | Expected | Observed | Expected | Observed |
| NCOGC | 25.2 | 7 | 26.2 | 7 | 26.2 | 8 |
| Single CO | 22.1 | 20 | 23 | 27 | 23.0 | 23 |
| Double CO | 2.7 | 15 | 2.8 | 4 | 2.8 | 6 |
| Triple CO | 0.1 | 4 | 0.1 | 1 | 0.1 | 0 |
| Quadruple CO | 0 | 2 | 0 | 0 | 0 | 0 |

Total observed CO and NCOGC frequencies are significantly different than expected based on wild-type frequencies ($p < 0.05$; Fisher's exact test; both chromosomes). Expected numbers were calculated using wild-type frequencies from [7].

larger increases in the centromere-proximal and subtelomeric regions (Figure 1B). It is tempting to speculate that structural differences between the chromosomes cause different strengths in their response. Centromeric suppression of COs is much weaker on the X chromosome due to a large block of heterochromatin [7, 8], potentially making it easier to increase the CO rate in that region during the IC effect. Similarly different degrees of responses are also reported in the historical literature on the IC effect [1] and have been observed in natural populations [9].

COs in *D. melanogaster* are typically limited to an average of one CO per chromosome arm by CO patterning mechanisms. One of these mechanisms is CO interference, which prevents COs from occurring close to each other and ultimately results in a non-random distribution of COs along a chromosome [10]. On the X chromosome, the increase in CO frequency results in the recovery of significantly more double CO (DCO) chromosomes than expected ($p < 0.001$; chi-square test), as well as several triple and quadruple COs (Table 1; Figure S2), which in wild-type are recovered at rates fewer than 1 in 1,000 or 1 in 10,000, respectively [11]. An increase in frequency of multi-CO chromosomes could indicate a loss or weakening of CO interference. We modeled CO interference by calculating the average physical pairwise distance between single COs in wild-type and compared that to the observed distances between DCOs (Figure 1C; STAR Methods). For all three chromosome arms, DCO distances are significantly greater than expected by chance ($p < 0.001$), showing that interference is still intact. For the X chromosome, DCO distances are not significantly different than distances observed in wild-type; however, for chromosome 2, the observed DCO distances are shorter than in wild-type (Figure 1C), suggesting that interference may be weaker, but not absent, during the IC effect on this chromosome. Together, these data show that interference is largely intact in the presence of a heterozygous inversion and that chromosome arms can accommodate more than one CO while still maintaining interference.

One possible mechanism for increasing CO frequency is to make more double-strand breaks (DSBs). Alternatively, the number of DSBs could remain the same, but a higher proportion of those DSBs could be repaired as COs at the expense of NCOGCs. We tested both of these hypotheses by examining the number of NCOGCs that occurred on the freely recombining chromosomes (Figure 1D; Data S1). We found that, for both chromosomes, we recovered significantly fewer NCOGCs than expected (Table 1). Additionally, using maximum-likelihood analysis, we estimate a rate of $1.4 \times 10^{-8}$ NCOGCs per base pair per generation for the freely recombining 2nd chromosome and $1.9 \times 10^{-8}$ for the freely recombining X chromosome, rates that are approximately 65% and 89% of the wild-type genome-wide estimate of $2.1 \times 10^{-8}$ using the same method [7]. The pattern of NCOGCs for chromosomes *2L* and *2R* show a uniform decrease in rates across the chromosome, yet the pattern of NCOGCs for the X chromosome shows large decreases in rate for some regions and increases for others, potentially explaining why the per base pair rate of NCOGC is closer to wild-type for the X chromosome. Thus, the frequency of COs on freely recombining chromosomes increases in response to heterozygous inversions, yet there appears to be no corresponding increase in the rate of NCOGCs.

We next analyzed the relationship between COs and NCOGCs on the inverted chromosomes. We identified 78 NCOGC events between the 2nd and 3rd chromosome balancers and their structurally linear homologs (Figure 2; Data S1). Using maximum-likelihood analysis, we estimate a NCOGC rate between these multiply inverted chromosomes and their homologs of $3.0 \times 10^{-8}$ per base pair per generation, a rate approximately 40% higher than wild-type. These data suggest that DSBs on inversion chromosomes are preferentially repaired as NCOGCs. We have, however, also considered the possibility that the NCOGC rate is higher on inversion chromosomes due to preferential recovery of non-exchange chromosomes. Sturtevant and Beadle demonstrated that COs within paracentric inversions do not affect viability and are most likely segregated into polar

(B) Per-arm CO frequency and distribution. Frequency is reported as cM/Mb using a 500-kb sliding window with a best-fit line. Wild-type data (blue) are from [3]; data from this study are shown in green. Some, but not all, centromere-proximal heterochromatin is included in the *D. melanogaster* release 6 assembly and is shaded in gray. Centromeres are represented as black circles on the x axes.

(C) Models of CO interference. Vertical lines represent observed distances between DCOs in wild-type (blue) and during the IC effect (green).

(D) Per-arm NCOGC frequency and distribution. Frequency is reported as number of events per 1 Mb using a 500-kb sliding window with a best-fit line. Wild-type data from [3] are in blue; data from this study are in green.

See also Figure S1 and Data S1.

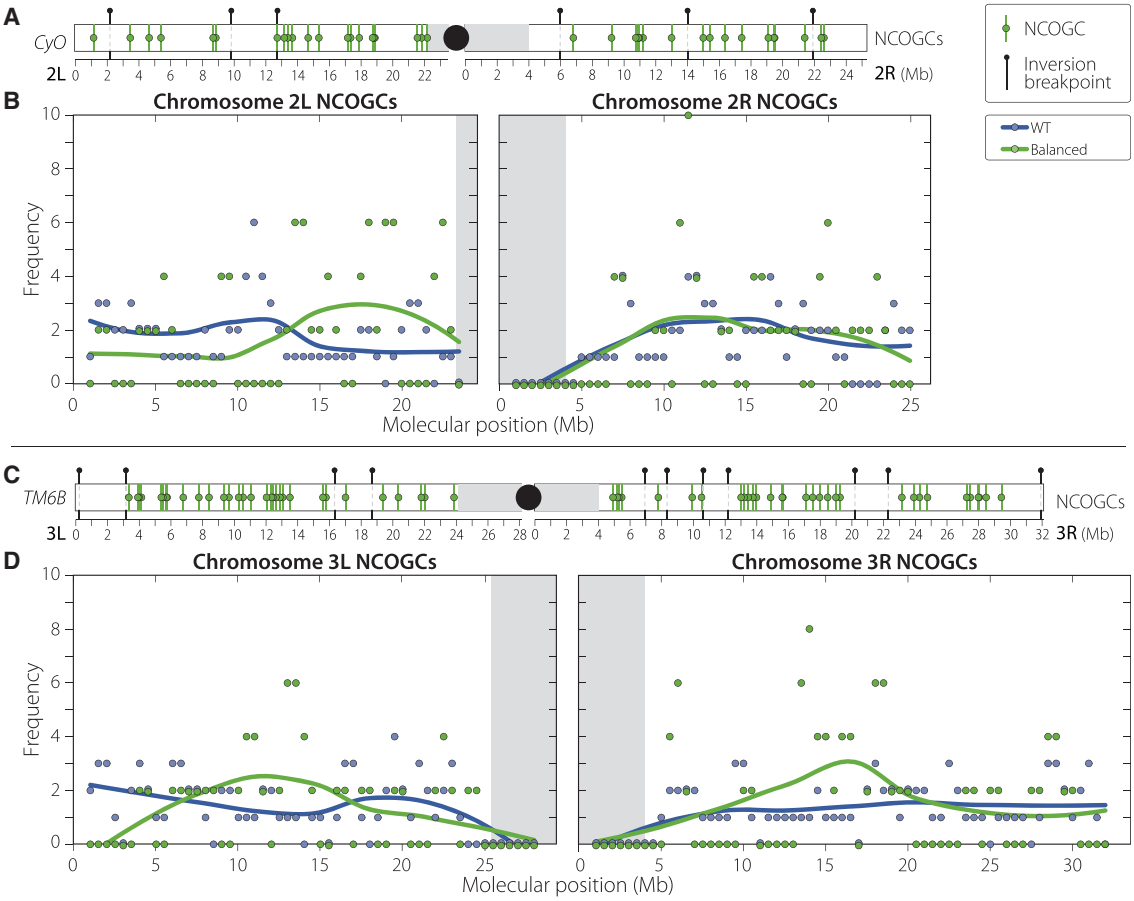


**Figure 2. The Frequency and Distribution of NCOGCs on Multiply Inverted Balancer Chromosomes**

(A) Location of NCOGCs onto the multiply inverted 2nd chromosome balancer *CyO*.

(B) Per-arm NCOGC frequency and distribution for the multiply inverted 2nd chromosome balancer *CyO*. Frequency is reported as number of events per 1 Mb using a 500 kb sliding window with a best-fit line. Some centromere-proximal heterochromatin is included in the release 6 assembly and is shaded in gray.

(C) Location of NCOGCs onto the multiply inverted 3rd chromosome balancer *TM6B*. Heterochromatin is shaded in gray.

(D) Per-arm NCOGC frequency and distribution for the multiply inverted 3rd chromosome balancer *TM6B*. Frequency is reported as number of events per 1 Mb using a 500 kb sliding window with a best-fit line.

See also Figure S2 and Data S1.

bodies, supporting the possibility that transmission distortion is responsible for the increase in NCOGCs in the present study [12]. However, cytological studies of the X chromosome balancer FM7 (which contains only paracentric inversions) have demonstrated that these chromosomes are rarely linked by chiasmata at metaphase, arguing that DSBs on these chromosomes are rarely repaired as COs and that exchange is truly suppressed [13, 14]. COs within pericentric inversions (as are found on 2nd and 3rd chromosomal balancers) result in lethal duplications and deletions but are predicted to segregate normally. However, there are genetic data showing that pericentric inversions surprisingly do not decrease viability but rather that the frequency of COs within pericentric inversions is reduced to 25% of wild-type [15, 16]. Thus, balancers comprising paracentric and those comprising pericentric inversions prevent the recovery of COs primarily by reducing exchange rather than reducing the recovery of exchanges. Therefore, although transmission distortion may be contributing to the increase in NCOGCs in the present study, we believe the effect is largely due to preferential repair of DSBs into NCOGCs.

There is mounting evidence that, in *Drosophila* species, inversion breakpoints suppress COs 1–3 Mb outside the breakpoint [2, 3, 5, 6, 17]; this type of suppression is mechanistically distinct from the transmission distortion discussed above, as it extends outside of the inversion. Indeed, in this study, we recovered one single CO and one DCO that occurred between a balancer chromosome and its structurally linear homolog, with both events occurring no closer than 1.7 Mb from the nearest inversion breakpoint (Figure S2; Data S1). It has remained unclear whether NCOGCs are similarly suppressed near inversion breakpoints. We analyzed the distances between inversion breakpoints and NCOGCs and found that 21 NCOGCs occurred within 1 Mb of an inversion breakpoint. Of those 21 NCOGCS, only 3 were within 500 kb of the breakpoints (Figure S3). Although these data suggest that NCOGCs may be suppressed very locally around inversion breakpoints, overall they are clearly less

**Table 2. Calculation of Number of DSBs per Meiosis Using NCOGC and CO Rates in Wild-Type and during the Interchromosomal Effect**

| | Wild-Type | Interchromosomal Effect |
|---|---|---|
| Stocks sequenced | 196 | 50 |
| NCOGCs | | |
| NCOGC rate[a] | 2.10E−08 | 1.86E−08 (X chromosome); 2.95E−08 (2nd and 3rd chromosomes) |
| NCOGCs per haploid meiosis[b] | 2.8 | 0.44 (X chromosome); 3.2 (2nd and 3rd chromosomes) |
| DSBs this accounts for per meiosis[c] | 11.1 | 1.76 (X chromosome DSBs); 12.9 (2nd and 3rd chromosome DSBs) |
| COs | | |
| Total COs observed | 541 | 70 (X chromosome) |
| DSBs this accounts for per meiosis[d] | 5.5 | 2.8 |
| Total breaks[e] | 16.6 | 17.5 |

For simplicity, data from the *CyO; TM6B* crosses are used to calculate number of DSBs during the IC effect (i.e., COs observed on the normal sequence X chromosome, the NCOGC rate for the X chromosome, and the combined NCOGC rate for *CyO* and *TM6B*). The genome-wide number of COs and NCOGC rate is used for the wild-type. See also Figures 1 and 2.

[a]NCOGC rates are maximum-likelihood estimates. See STAR Methods for a description.

[b]Calculated by multiplying the NCOGC rate per base pair by the genome size in base pairs.

[c]Calculated by multiplying the NCOGCs per haploid meiosis by four, as only one-quarter of NCOGCs are detected.

[d]Calculated by multiplying the number of crossovers by two, as only one-half of CO events are observed, then dividing by the number of stocks sequenced.

[e]Calculated by adding DSBs repaired as NCOGCs and those repaired as COs.

sensitive to the mechanisms that suppress CO formation 1–3 Mb around inversion breakpoints.

The most parsimonious explanation for the genome-wide changes in CO and NCOGC frequencies during the IC effect is that the total DSB number is approximately the same as in wild-type. Cytological studies in *D. melanogaster* have demonstrated that 20–25 DSBs are made during female meiosis and that this number does not increase in the presence of multiple balancer chromosomes [18, 19]. However, the average number of DSBs can also be estimated from our data. Using the NCOGC rate in inversions and the CO and NCOGC rates on freely recombining chromosomes, we calculate that 17.5 DSBs were made per genome per meiosis (Table 2; this calculation corrects for the fact that only one-quarter of the NCOGCs and one-half of COs are recovered in the progeny). We used the same analysis on wild-type data [7] and, strikingly, calculated that 16.6 DSBs are made per genome per meiosis (Table 2). The calculated number of DSBs in each experiment is 10%–20% smaller than cytological estimates, potentially because of genetically invisible events, such as noncrossover gene restorations or intersister recombination. Indeed, the ability to adjust the ratio of COs to NCOGCs is reminiscent of CO homeostasis in budding yeast and mice, where if the number of DSBs is decreased, the number of COs is generally maintained at the expense of NCOGCs [20, 21].

Our data lead to a model where the recombination landscape in *D. melanogaster* responds to heterozygous inversions by modifying the fate of DSBs, not by increasing the number of DSBs. Furthermore, most of this shift occurs in subtelomeric and centromere proximal regions, where CO control mechanisms normally favor NCOGC formation [7]. Recent evidence has shown that the number of DSBs formed during meiosis is controlled using multiple feedback mechanisms. In several organisms, including *D. melanogaster*, there is a DSB-limiting mechanism that shuts down DSB formation [22, 23]. In budding yeast, there is also a feedback mechanism that increases the number of DSBs made in response to problems with "homolog engagement" [24]. Although the IC effect has been compared to problems with homolog engagement by others [24], cytological examination of phosphorylated H2AV, a marker of DSBs, and our maximum-likelihood estimates presented here suggest that DSBs never accumulate to levels higher than wild-type [18]. Thus, a comprehensive assessment of the data suggests that the increase in COs during the IC effect is not due to an increase in DSB number.

It is intriguing to consider how the IC effect might cause this change in DSB fate. One current model is that chromosome axis discontinuities between the inversion and its homolog trigger a checkpoint that extends the time during which DSBs can be repaired as COs [1, 18]. An alternative model is that the absence of a CO on the inverted chromosome triggers a CO assurance checkpoint. Until this checkpoint is satisfied, DSBs continue to be repaired as COs on the freely recombining chromosome. Because interference is still intact, COs in the medial part of the chromosome arm still prevent neighboring DSBs from being repaired as COs, but DSBs in the subtelomeric and centromere proximal regions are free to be repaired as COs. The latter model implies that NCOGC formation in subtelomeric and centromere-proximal regions is delayed until after CO formation is complete. Existing molecular evidence supports the idea that the final decision to repair a DSB as a CO or NCOGC is made late in the DNA repair process [25]; this late decision may provide flexibility in response to a CO assurance checkpoint. Interestingly, in many organisms, DSB repair is required for full chromosome pairing and formation of the synaptonemal complex (the tripartite structure formed between homologous chromosomes during meiosis) [26]. In *D. melanogaster*, chromosomes pair and synaptonemal complex is built before DSBs are

made [27]; therefore, DSBs most likely provide no advantage during homology searching. Our data lead us to believe that in *D. melanogaster*, where DSB repair is not required for homolog pairing, NCOGCs can function as a reserve of potential COs sites when the desired number of COs have not been formed.

Recombination, and particularly crossing over, is essential for proper chromosome segregation during meiosis, but it is also important for allowing genetic exchange among individuals, which ultimately homogenizes nucleotide diversity within or between populations. Depending on their frequency in a population, inversions can act as barriers to gene flow by suppressing COs and thus play an important role in sequestering haplotypes away from genetic exchange. This sequestration is essential for maintaining linkage and may be particularly important in cases when inversions harbor blocks of co-adapted alleles, such as supergenes [28] and meiotic drive systems [29], and is also a critical mode of speciation [30, 31]. Suppressing COs is effective at slowing gene flow at the megabase scale, but the rates of NCOGCs we have presented here would allow higher than wild-type rates of gene flow on a small scale (the average NCOGC size is 400 bp in *D. melanogaster*) [32]. We have shown that NCOGCs clearly happen throughout inversions, are insensitive to the mechanisms that suppress CO formation, and are transmitted at a rate approximately 40% higher than wild-type. Although NCOGCs are unlikely to completely break down linkage disequilibrium in an inversion, they will allow new genetic information in and out of the sequestered region. Therefore, although inversions may be maintained because of their ability to keep haplotypes together by suppressing COs, NCOGCs may be equally important for their persistence by allowing frequent but small amounts of gene flow. Our baseline estimate of the transmission rate of NCOGC frequency within inversions suggests that NCOGCs may cause faster homogenization of nucleotide diversity than is accounted for in current models and at least necessitates a re-examination of those models [33].

Together, our data lead to a comprehensive model of how inversions act both in *cis* and *trans* to change the global landscape of recombination in *D. melanogaster.* Locally, they prevent DSBs from being repaired as COs but have no negative effect on NCOGCs, and globally, they cause an increase in COs and a decrease in NCOGCs on freely recombining chromosomes. Thus, the net effect of heterozygous inversions in *D. melanogaster* is not just local suppression of COs but a genome-wide shift in the distribution of large-scale genetic exchange. Such dramatic changes to the pattern of gene flow across genomes will have an impact on the dynamics of population genetics and are especially important to consider when modeling the contributions of inversions to speciation or ecological adaptation.

## STAR★METHODS

Detailed methods are provided in the online version of this paper and include the following:

- KEY RESOURCES TABLE
- CONTACT FOR REAGENT AND RESOURCE SHARING
- EXPERIMENTAL MODEL AND SUBJECT DETAILS
- METHOD DETAILS
  - DNA isolation, sequencing, genome alignment, and SNP calling
  - Sanger sequencing of individual NCOGCs
- QUANTIFICATION AND STATISTICAL ANALYSIS
  - Identification of CO and NCOGC events
  - Calculation of CO and NCOGC rates
  - Modeling of interference
- DATA AND SOFTWARE AVAILABILITY

## SUPPLEMENTAL INFORMATION

Supplemental Information includes three figures, three tables, and one data file and can be found with this article online at https://doi.org/10.1016/j.cub.2018.07.004.

## ACKNOWLEDGMENTS

We thank Justin Blumenstiel, Mohamed Noor, Katharine Korunes, and members of the Hawley, Sekelsky, and Zanders labs for helpful comments and discussion; Angela Miller for help with figure preparation and editing; and members of the Stowers Institute Molecular Biology core for expert help with DNA sequencing. K.N.C. is supported by NIH grant 5K99GM118826. J.S. is supported by NIH grant 1R35GM118127. R.S.H. is supported by the Stowers Institute for Medical Research. This research was funded by an award to R.S.H. from the Stowers Institute for Medical Research and NIH grant 5K99GM118826 to K.N.C. The following ORCIDs apply to the authors: 0000-0002-2595-3428 (K.N.C.), 0000-0001-6096-8601 (D.E.M.), 0000-0002-4424-677X (J.S.), and 0000-0002-6478-0494 (R.S.H.).

## AUTHOR CONTRIBUTIONS

K.N.C. was responsible for conceptualization, methodology, investigation, and writing. D.E.M. was responsible for conceptualization, methodology, software, investigation, and writing. J.S. and R.S.H. were responsible for conceptualization.

## DECLARATION OF INTERESTS

The authors declare no competing interests.

Received: March 22, 2018
Revised: June 6, 2018
Accepted: July 2, 2018
Published: August 30, 2018

## REFERENCES

1. Lucchesi, J.C., and Suzuki, D.T. (1968). The interchromosomal control of recombination. Annu. Rev. Genet. *2*, 53–86.
2. Stevison, L.S., Hoehn, K.B., and Noor, M.A.F. (2011). Effects of inversions on within- and between-species recombination and divergence. Genome Biol. Evol. *3*, 830–841.
3. Miller, D.E., Cook, K.R., Hemenway, E.A., Fang, V., Miller, A.L., Hales, K.G., and Hawley, R.S. (2018). The molecular and genetic characterization of second chromosome balancers in *Drosophila melanogaster*. G3 (Bethesda) *8*, 1161–1171.
4. Lindsley, D.L., and Zimm, G.G. (1992). The Genome of Drosophila melanogaster (Academic Press).
5. Miller, D.E., Cook, K.R., Arvanitakis, A.V., and Hawley, R.S. (2016). Third chromosome balancer inversions disrupt protein-coding genes and influence distal recombination events in Drosophila melanogaster. G3 (Bethesda) *6*, 1959–1967.
6. Miller, D.E., Cook, K.R., Yeganeh Kazemi, N., Smith, C.B., Cockrell, A.J., Hawley, R.S., and Bergman, C.M. (2016). Rare recombination events

generate sequence diversity among balancer chromosomes in Drosophila melanogaster. Proc. Natl. Acad. Sci. USA *113*, E1352–E1361.

7. Miller, D.E., Smith, C.B., Kazemi, N.Y., Cockrell, A.J., Arvanitakas, A.V., Blumenstiel, J.P., Jaspersen, S.L., and Hawley, R.S. (2016). Whole-genome analysis of individual meiotic events in Drosophila melanogaster reveals that noncrossover gene conversions are insensitive to interference and the centromere effect. Genetics *203*, 159–171.
8. Yamamoto, M., and Miklos, G.L.G. (1978). Genetic studies on heterochromatin in Drosophila melanogaster and their implications for the functions of satellite DNA. Chromosoma *66*, 71–98.
9. Hunter, C.M., Huang, W., Mackay, T.F.C., and Singh, N.D. (2016). The genetic architecture of natural variation in recombination rate in Drosophila melanogaster. PLoS Genet. *12*, e1005951.
10. Lake, C.M., and Hawley, R.S. (2012). The molecular control of meiotic chromosomal behavior: events in early meiotic prophase in Drosophila oocytes. In Annual Review of Physiology, *Volume 74*, D. Julius, and D.E. Clapham, eds. (Annual Reviews), pp. 425–451.
11. Weinstein, A. (1936). The theory of multiple-strand crossing over. Genetics *21*, 155–199.
12. Sturtevant, A.H., and Beadle, G.W. (1936). The relations of inversions in the X chromosome of Drosophila melanogaster to crossing over and disjunction. Genetics *21*, 554–604.
13. Gong, W.J., McKim, K.S., and Hawley, R.S. (2005). All paired up with no place to go: pairing, synapsis, and DSB formation in a balancer heterozygote. PLoS Genet. *1*, e67.
14. Theurkauf, W.E., and Hawley, R.S. (1992). Meiotic spindle assembly in Drosophila females: behavior of nonexchange chromosomes and the effects of mutations in the nod kinesin-like protein. J. Cell Biol. *116*, 1167–1180.
15. Coyne, J.A., Meyers, W., Crittenden, A.P., and Sniegowski, P. (1993). The fertility effects of pericentric inversions in Drosophila melanogaster. Genetics *134*, 487–496.
16. Navarro, A., and Ruiz, A. (1997). On the fertility effects of pericentric inversions. Genetics *147*, 931–933.
17. McGaugh, S.E., and Noor, M.A.F. (2012). Genomic impacts of chromosomal inversions in parapatric Drosophila species. Philos. Trans. R. Soc. Lond. B Biol. Sci. *367*, 422–429.
18. Joyce, E.F., and McKim, K.S. (2010). Chromosome axis defects induce a checkpoint-mediated delay and interchromosomal effect on crossing over during Drosophila meiosis. PLoS Genet. *6*, 15.
19. Mehrotra, S., and McKim, K.S. (2006). Temporal analysis of meiotic DNA double-strand break formation and repair in Drosophila females. PLoS Genet. *2*, e200.
20. Cole, F., Kauppi, L., Lange, J., Roig, I., Wang, R., Keeney, S., and Jasin, M. (2012). Homeostatic control of recombination is implemented progressively in mouse meiosis. Nat. Cell Biol. *14*, 424–430.
21. Martini, E., Diaz, R.L., Hunter, N., and Keeney, S. (2006). Crossover homeostasis in yeast meiosis. Cell *126*, 285–295.
22. Joyce, E.F., Pedersen, M., Tiong, S., White-Brown, S.K., Paul, A., Campbell, S.D., and McKim, K.S. (2011). Drosophila ATM and ATR have distinct activities in the regulation of meiotic DNA damage and repair. J. Cell Biol. *195*, 359–367.
23. Lange, J., Pan, J., Cole, F., Thelen, M.P., Jasin, M., and Keeney, S. (2011). ATM controls meiotic double-strand-break formation. Nature *479*, 237–240.
24. Thacker, D., Mohibullah, N., Zhu, X., and Keeney, S. (2014). Homologue engagement controls meiotic DNA break number and distribution. Nature *510*, 241–246.
25. Crown, K.N., McMahan, S., and Sekelsky, J. (2014). Eliminating both canonical and short-patch mismatch repair in Drosophila melanogaster suggests a new meiotic recombination model. PLoS Genet. *10*, e1004583.
26. Kauppi, L., Barchi, M., Lange, J., Baudat, F., Jasin, M., and Keeney, S. (2013). Numerical constraints and feedback control of double-strand breaks in mouse meiosis. Genes Dev. *27*, 873–886.
27. McKim, K.S., Green-Marroquin, B.L., Sekelsky, J.J., Chin, G., Steinberg, C., Khodosh, R., and Hawley, R.S. (1998). Meiotic synapsis in the absence of recombination. Science *279*, 876–878.
28. Joron, M., Frezal, L., Jones, R.T., Chamberlain, N.L., Lee, S.F., Haag, C.R., Whibley, A., Becuwe, M., Baxter, S.W., Ferguson, L., et al. (2011). Chromosomal rearrangements maintain a polymorphic supergene controlling butterfly mimicry. Nature *477*, 203–206.
29. Larracuente, A.M., and Presgraves, D.C. (2012). The selfish Segregation Distorter gene complex of Drosophila melanogaster. Genetics *192*, 33–53.
30. Noor, M.A.F., Grams, K.L., Bertucci, L.A., and Reiland, J. (2001). Chromosomal inversions and the reproductive isolation of species. Proc. Natl. Acad. Sci. USA *98*, 12084–12088.
31. Rieseberg, L.H. (2001). Chromosomal rearrangements and speciation. Trends Ecol. Evol. *16*, 351–358.
32. Hilliker, A.J., Harauz, G., Reaume, A.G., Gray, M., Clark, S.H., and Chovnick, A. (1994). Meiotic gene conversion tract length distribution within the *rosy* locus of *Drosophila melanogaster*. Genetics *137*, 1019–1026.
33. Navarro, A., and Barton, N.H. (2003). Accumulating postzygotic isolation genes in parapatry: a new twist on chromosomal speciation. Evolution *57*, 447–459.
34. Li, H., and Durbin, R. (2009). Fast and accurate short read alignment with Burrows-Wheeler transform. Bioinformatics *25*, 1754–1760.
35. Smit, A.F.A., Hubley, R., and Green, P. (2015). RepeatMasker Open-4.0 (Institute for Systems Biology).
36. Robinson, J.T., Thorvaldsdóttir, H., Winckler, W., Guttman, M., Lander, E.S., Getz, G., and Mesirov, J.P. (2011). Integrative genomics viewer. Nat. Biotechnol. *29*, 24–26.
37. Hoskins, R.A., Carlson, J.W., Wan, K.H., Park, S., Mendez, I., Galle, S.E., Booth, B.W., Pfeiffer, B.D., George, R.A., Svirskas, R., et al. (2015). The Release 6 reference sequence of the Drosophila melanogaster genome. Genome Res. *25*, 445–458.

# STAR★METHODS

## KEY RESOURCES TABLE

| REAGENT or RESOURCE | SOURCE | IDENTIFIER |
|---|---|---|
| Critical Commercial Assays | | |
| DNeasy Blood and Tissue Kit | QIAGEN | 69506 |
| KAPA HTP Library Prep kit | KAPA | KK8234 |
| NEXTflex DNA barcodes | BI00 Scientific | NOVA-514104 |
| Primestar GXL Polymerase | Takara Clontech | R050A |
| GeneJet PCR Purification Kit | ThermoFisher Scientific | 0701 |
| Deposited Data | | |
| Illumina sequencing reads | NCBI | PRJNA432528 |
| Experimental Models: Organisms/Strains | | |
| *D. melanogaster* $w^{1118}$ | RSH lab | N/A |
| *D. melanogaster Oregon-RM* | RSH lab | N/A |
| *D. melanogaster y; cn bw sp (ISO-1 reference genome)* | RSH lab | N/A |
| *D. melanogaster FM7w* | JS lab | N/A |
| *D. melanogaster CyO* | JS lab | N/A |
| *D. melanogaster TM6B Tb Hu* | JS lab | N/A |
| Oligonucleotides | | |
| See Table S3 | N/A | N/A |
| Software and Algorithms | | |
| BWA version 0.7.15-r1140 | [34] | http://bio-bwa.sourceforge.net/ |
| SAMtools version 1.3.1 | [34] | http://samtools.sourceforge.net/ |
| repeatmasker | [35] | http://www.repeatmasker.org/ |
| Mathematica | Wolfram | http://www.wolfram.com/mathematica |
| R | N/A | https://www.r-project.org/ |
| Integrated Genome Viewer | [36] | http://software.broadinstitute.org/software/igv/ |

## CONTACT FOR REAGENT AND RESOURCE SHARING

Further information and requests for resources and reagents should be directed to and will be fulfilled by the Lead Contact, Scott Hawley (rsh@stowers.org).

## EXPERIMENTAL MODEL AND SUBJECT DETAILS

Crosses used to create the double-balanced females used in this study are shown in Figure 1A. The laboratory $w^{1118}$, *Oregon-R, ISO-1*, *FM7w*, *TM6B* and *CyO* stocks used in this study have been maintained in the labs of RSH and JS separately from the Bloomington *Drosophila* Stock Center, and are available upon request. The wild-type data used in this study were previously published in [3] and were from a $w^{1118}$/*Canton-S* background. Crosses for the wild-type data and this data were maintained at 25 degrees on standard medium.

## METHOD DETAILS

### DNA isolation, sequencing, genome alignment, and SNP calling

DNA was isolated from either 10 females from each of the parental lines or single males or females for individual offspring (Table S1). Flies were frozen at –80 C for at least 1 hr before DNA extraction using the QIAGEN Blood and Tissue kit following the manufacturer instructions. A Covaris S220 sonicator was used to shear genomic DNA and a Perkin Elmer Sciclone G3 NGS Workstation was used

to construct libraries using the KAPA HTP Library Prep kit (KAPA Biosystems, Cat. No. KK8234) using NEXTflex DNA barcodes (Bioo Scientific, Cat No. NOVA-514104). A Pippin Prep (Sage Science) was used for library size selection post-amplification and libraries were pooled after quantification with an Invitrogen Qubit 2.0 Fluorometer and an Agilent 2100 Bioanalyzer. Sequencing was performed on an Illumina NextSeq 500 instrument as 150 bp on a high-output, paired-end flow cell. Illumina NextSeq Real Time Analysis version 2.4.11 and bcl2fastq2 v2.18 were run to demultiplex reads and generate FASTQ files. Bwa version 0.7.15-r1140 [34] was used to align reads to release 6 (dm6) of the *Drosophila melanogaster* genome and SNPs were called using SAMtools mpileup [34]. For Figures 1 and 2, heterochromatin is defined computationally as highly repetitive regions near the centromere that are assembled in release 6 of the *Drosophila* genome [37].

### Sanger sequencing of individual NCOGCs

Twenty random NCOGC events were chosen for confirmation by Sanger sequencing. Primers were designed using Primer3 to amplify 500-1600 bases around the NCOGC event. Polymerase chain reaction (PCR) was carried out using DNA from the same DNA isolation used in whole genome sequencing described above. All PCR reactions contained: 0.5 μL Primestar GXL Polymerase (Takara Clontech #R050A), 5 μL Primerstar GXL Reaction Buffer, 0.5 μL each primer (primers resuspended at 50 uM), 0.5 μL 10 mM dNTPs, 2-10 ng DNA, water to 25 μL total volume. Reactions were run on a 1% agarose gel and gel purified using 600 μL Buffer QG (QIAGEN #19063) and a GeneJet PCR Purification Kit (ThermoFisher Scientific #0701). PCR products were sent to EtonBio for standard Sanger sequencing. All 20 events were confirmed as real.

## QUANTIFICATION AND STATISTICAL ANALYSIS

### Identification of CO and NCOGC events

Crossover (CO) and noncrossover gene conversion (NCOGC) events were identified as in [3] using custom scripts available at the link below. Briefly, to identify CO and NCOGC events onto chromosomes able to undergo exchange, the SNPs in each parental genotype were called (either *Oregon-R* and *ISO-1* for the X chromosome and *Oregon-R* or $w^{1118}$ for the 2$^{nd}$ chromosome). For the *X*, only homozygous parental *Oregon-R* SNPs were used while only SNPs heterozygous between *Oregon-R* and $w^{1118}$ were used for the 2$^{nd}$. Repetitive regions were masked as defined by repeatmasker [35]. For both classes only parental SNPs with quality scores >150 that were unique between the parents were used in order to determine where, if anywhere, in the offspring the parental genotype changed. Only SNPs in the offspring with quality scores >220 were considered and each change in genotype flagged by our script was confirmed by visual analysis.

To identify COs and NCOGCs onto the *CyO* or *TM6B* balancer chromosomes, we identified either SNPs or loss of a SNP for each balancer that were unique among all the balancer chromosomes sequenced. For example, 50 *CyO* chromosomes were sequenced as *CyO/ISO-1*, so only unique SNPs, or loss of a SNP, present in 1 of 49 individuals was considered a candidate NCOGC event. Each potential NCOGC and CO was visually validated using IGV [36] by confirming that the SNP or loss of SNP was consistent with the sequence of the non-inverted homolog.

### Calculation of CO and NCOGC rates

For all analyses, 2L and 2R were treated as independent chromosomes because CO control mechanisms act independently on individual arms. CO rates were calculated as the number of COs occurring per 1 Mb using a 500 kb sliding window. Changing the size of the sliding window to either 250 kb or 1 Mb did not change the statistical significance of the data. NCOGC rate was estimated using maximum-likelihood analysis as in [7]. Briefly, for each calculation observed, NCOGCs were fit to the actual SNP distributions from respective chromosome arms. SNP distributions for each chromosome arm were collected by counting the number of intervals in which a single bp separated two SNPs, then the intervals in which 2 bp separated two SNPs, until all intervals up to 10,000 bp between SNPs had been counted. For each trial, tract lengths of 100–500 bp were tested in increments of 5 bp using five different DSB rates from $1.0 \times 10^{-7}$ to $4.0 \times 10^{-8}$. A local maximum was identified, and then tract length and rate were reset and re-run in smaller increments until the true local maximum was identified. Mathematica scripts of each model are available at the link below.

### Modeling of interference

Interference for the X and 2$^{nd}$ chromosomes was modeled independently by performing 100,000 trials of randomly selecting two single crossover (SCO) events from wild-type reported in [7] and measuring the distance between them. The wild-type pool of SCOs selected from was not significantly different from the SCOs recovered in this study (two-sample Kolmogorov-Smirnov p value 0.28 for the X chromosome, 0.72 for chromosome *2L*, and 0.84 for chromosome *2R*). We then compared the average distance between double crossovers (DCOs) for the *X*, *2L*, and *2R* independently to the SCOs from the respective chromosomes. A p value was calculated by comparing the observed DCO size to the average DCO size obtained by bootstrapping (X chromosome expected 5,735,929 bp, observed 8,478,101; chromosome *2L* expected 5,469,470 bp, observed 9,811,734; chromosome *2R* expected 5,018,928 bp, observed 8,448,263). The strength of interference was determined by comparing wild-type data to the DCO data obtained by bootstrapping SCO events. The distance between two randomly selected SCO events was used to construct a histogram

using a bin size of 100 kb from which a best-fit curve was derived. The average value between observed DCOs in this study was then plotted and compared to the average value between observed DCOs in [7]. For all observations, any triple crossover (TCO) was treated as two DCOs and any quadruple crossover (QCO) was treated as three DCOs.

## DATA AND SOFTWARE AVAILABILITY

The accession number for all sequencing data reported in this paper is NCBI: PRJNA432528. Scripts used to identify CO and NCOGC events can be found on GitHub at https://github.com/danrdanny/interChromosomalEffect. Original data underlying this manuscript can be accessed from the Stowers Original Data Repository at http://www.stowers.org/research/publications/libpb-1283.